ELSEVIER

Inorganica Chimica Acta 243 (1996) 229–232

Inorganica Chimica Acta

X-Ray magnetic circular dichroism at temperatures <1 K: demonstration with the blue copper site in plastocyanin[1]

Jason Christiansen[a], Gang Peng[a], Anthony T. Young[b], Louis B. LaCroix[c], Edward I. Solomon[c], Stephen P. Cramer[a,b,*]

[a]*Department of Applied Science, University of California at Davis, Davis, CA 95616, USA*
[b]*Energy and Environment Division, Lawrence Berkeley Laboratory, Berkeley, CA 94720, USA*
[c]*Department of Chemistry, Stanford University, Stanford, CA 94305, USA*

Abstract

We have demonstrated the first XMCD to be taken at ultra-low temperatures (<1 K) using a ^{3}He cryostat. By measuring the XMCD at a fixed temperature and varying fields, we have been able to plot a magnetization curve for the $S = 1/2$ Cu site in the protein plastocyanin. This magnetization curve allows us to definitively calculate the temperature at the surface of the sample and remove any ambiguity related to the system thermometry. These experiments at low temperature open the door to further study of more complicated systems by optimizing the observable XMCD effect and allowing us to reach a wide range of field and temperature combinations.

Keywords: X-Ray magnetic circular dichroism; Blue copper protein; Plastocyanin

1. Introduction

X-Ray magnetic circular dichroism (XMCD) is the differential absorption of left and right circularly polarized X-rays in the presence of a magnetic field. This technique can provide element and oxidation state specific information about the magnetic properties of isolated metal centers, complex clusters, or multilayers. As the number of synchrotron sources capable of providing high photon flux and variable photon helicity grows, the XMCD technique is getting an increased amount of attention.

XMCD was first predicted for the $M_{4,5}$ edges of rare earth elements [1] and a linear dichroism effect was demonstrated experimentally at the Tb edge in a terbium-iron garnet [2]. The theory was then used to predict XMCD for the 3d transition metal $L_{2,3}$ edges [1,3] and demonstrated for several ferromagnetic and ferrimagnetic systems [4]. Soft XMCD was first demonstrated for a paramagnetic, biological system by probing the Fe site of rubredoxin from *Pyrococcus furiosus* [5]. Unlike the ferromagnetic or ferrimagnetic systems studied previously, a paramagnetic system requires a much stronger field and lower temperature to align the bulk magnetic moment of the sample.

The blue copper protein, plastocyanin, has been the subject of intense interest and study due to its importance in biological systems as an electron transferase [6]. The active site consists of Cu in a C_{3v} distorted T_d geometry [7] with a short thiolate S(cys)–Cu (2.07Å), a long thioether S(met)–Cu (2.82Å), and two normal N(his)–Cu (~2 Å) bonds [8]. It exhibits unique spectral features, including an intense blue color which Gray and co-workers [9] predicted to be a S(cys)–Cu charge transfer transition in a distorted tetrahedral site. These unique spectral features have been shown to arise from a highly covalent site [10]. More recently, Cu L-edge XAS has been used to quantify the high covalency of the copper site [11]. Using a sum rule relating the integrated L-edge intensity to the number of d vacancies, it was shown that about half of the formal d vacancy is filled by charge transfer from the ligands.

Other sum rules developed by Carra [12], Thole [13] and Altarelli [14] relate the integrated XMCD intensity to the orbital angular momentum. Plastocyanin is an ideal candidate for testing these sum rules, since it consists of a

* Corresponding author.

[1] This paper is dedicated to Professor Harry B. Gray.

0020-1693/96/$15.00
PII: S0020-1693(96)04912-2

single paramagnetic $S = 1/2$ Cu center with well understood electronic structure. The sample concentration is sufficient for good signal to noise. Furthermore, Arrio and co-workers [15] have developed analytical expressions that relate the XMCD to crystal field strength and spin-orbit splittings.

In this paper, we present the first XMCD experiments performed at very low temperatures, using the copper site in plastocyanin as a test system. By incorporating a ^{3}He cryostat into our split-coil superconducting magnet [16], we have been able to conduct XMCD experiments at temperatures <1 K, as demonstrated by the field dependence of the magnetization curve. The success of these experiments opens the door to further study of other complex metal clusters of both chemical and biological interest.

2. Experimental

2.1. Sample preparation

Plastocyanin was isolated from spinach by previously published methods [17] to a final concentration of ~0.8 mM in 250 mM potassium phosphate (pH 7) buffer. The sample was dehydrated onto a gold-plated, copper sample holder that was tightly screwed into a threaded opening with a tapered end on the sample cold finger. To guarantee good thermal contact, all copper contact points between the sample holder and cold finger were cleaned with an HCl/ZnCl flux to remove any oxide layers and thermally conductive grease was applied to the tapered end to ensure good contact at all points. During the experiment, the beam position on the sample was changed frequently, to minimize damage from photoreduction.

2.2. Experimental set-up

Experiments were conducted at the Stanford Synchrotron Radiation Laboratory on beamline 5–2 [18]. This beamline is ideal for these experiments due to the newly installed elliptically polarized undulator [19]. This insertion device is capable of producing the high brightness of an undulator, with the added advantage of being able to produce photons of left and right circular polarization, under control of the experimenter. In principle, only the photon helicity is changed as the insertion device magnet phase is swept, the beam path through the optics and the beam position on the sample are preserved throughout the experiment. This inherent stability eliminates any errors introduced by adjusting entrance slits or changing tilt of the entrance mirrors to swap polarization, as is typically done with bend magnet beamlines [20].

The XMCD apparatus used a superconducting split-coil magnet, enclosed in a UHV compatible chamber which connects directly with beamline vacuum to eliminate absorbing windows in the light path [16]. A windowless, liquid nitrogen cooled, 13 element solid-state Ge array detector [21] is inserted between the two coils, perpendicular to the photon beam path (Fig. 1). A ^{3}He cryostat is inserted from the top of the chamber and the cold finger sits at the center of the split between the two coils at a point of uniform field (Fig. 1).

The cryostat is a single-shot, pumped charcoal ^{3}He design [22] (Fig. 1, bottom right). The temperature of the sample cold finger is monitored by a Ge resistance thermometer located ~3 mm behind and ~5 mm above the center of the sample surface. This sensor indicated temperatures of ~0.3 K when the cryostat was fully cooled in the absence of a magnetic field. In order to shield the sample from heat sources, several shields were used (Fig. 1, top left). Surrounding the sample cold finger is an Al shield which is attached to the cryostat's liquid He reservoir which operates at 1.5 K, although higher temperatures were measured on the outside of the shield during the run. The front of this shield has a thin (1000 Å) Al window which lets the X-ray beam enter and the fluorescence emission exit to the Ge detector. There is a 50 Ω heater wrapped around the top of this shield to help prevent icing of the thin Al window during cooldown. There is another shield that surrounds approximately 80% of the 1.5 K shield that is connected to the magnet 4.2 K liquid He supply and can be dropped down to allow for optical access to the interior of the magnet bore. Viewports at the rear of the magnet and opposite the detector are sealed at

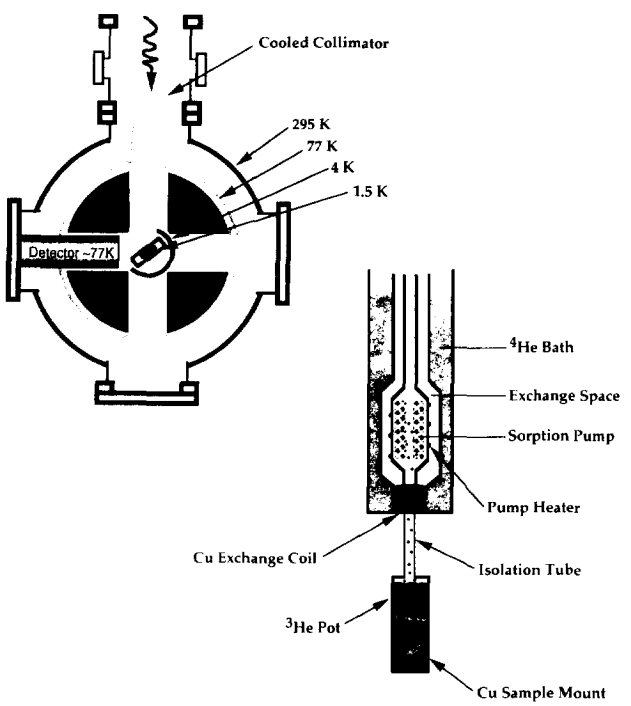

Fig. 1. Top, left: overhead schematic view of the magnet, detector and shielding layout. The sample is located in the very center, within the 1.5 K shielding. Bottom, right: schematic diagram of the ^{3}He cryostat and sample mount.

the liquid nitrogen shield by cooled quartz windows. Heat source input from the beampipe was minimized by attaching a liquid nitrogen cooled aluminum collimator with a 9.5 mm opening.

2.3. Data acquisition

Data were collected in two ways: spectral comparison and single energy counting. In both cases the detector amplifiers were set to 6 μs shaping time and count rates were kept in a linear range. For the spectral comparison method, the detector was set to count on the Cu L emission peak for the duration of the scan. Then, either the magnetic field or beam polarization was switched. Accompanying spectra taken without any magnetic field and alternating beam polarization were also taken to check for zero field effects and changes in energy calibration. All spectra for a given configuration were then compared for the presence of increased photoreduced Cu by examination of any baseline changes [11]. None of the spectra collected showed any evidence for a change in the amount of photoreduction in a data set. Spectra for each field and/or polarization were then compared and the peak integrated to get the total peak intensity and the resulting XMCD effect is reported as $I_l - I_r/I_l + I_r$.

The second method employed was that of single energy counting. In this configuration, the detector would accumulate counts for 120 s in two windows, one set for the O Kα and the other for the Cu L emission while the energy was fixed at 942 eV. The energy was then moved to 938 eV and a 'background' taken by accumulating counts as before. The ratio of these two (peak-baseline) signals at different fields and polarizations can then be used to calculate the XMCD effect at that single energy point.

3. Results and discussion

The XMCD in the L_3 edge of plastocyanin in a 1 T field is shown in Fig. 2. A strong, ~40% effect is clearly visible. (The rapidly rising baseline at the high energy side of the scan is due to transitions to 4s and continuum states and possibly to the presence of photoreduced protein. There were not any detectable changes in amplitude for all the scans used to generate these data. Since protein in the Cu(I) state does not contribute to the 2p $\rightarrow$ 3d L_3 transition, a modest fraction of photoreduced Cu(I) protein does not interfere with the magnetization curve measurements.) Data of this type was collected for several fields and the temperature was held fixed at a measured value of 0.3 K at the cold finger.

All of the data collected were then graphed on a magnetization plot showing the size of the effect versus the field/temperature ratio. For an isotropic $S = 1/2$ system, it has been shown that the XMCD should be of the form [23]

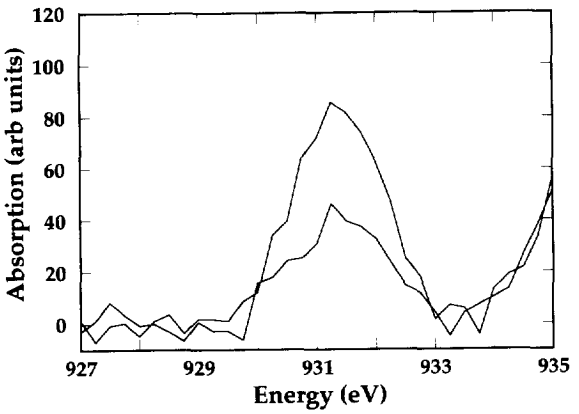

Fig. 2. A demonstration of the XMCD effect for a 1 T field and ~0.3 K. The two lines represent opposite beam helicity or opposite magnetic field.

$$\text{XMCD} = A\tanh\left[\frac{g\mu B}{2kT}\right] \quad (1)$$

where A is a normalization constant, μ/k is the ratio of the Bohr magneton and the Boltzmann constant, g is the electron g-factor (~2.00 for this case) and the ratio B/T is the field/temperature ratio. By fitting this functional form to the data with known B and optimized A and T, the temperature of the sample surface can be accurately determined. Knowledge of the true sample surface temperature is important, since temperature sensors located elsewhere within the system will probably monitor a lower temperature than that actually present on the surface. Due to their chemical composition, protein samples such as plastocyanin are not good thermal conductors, and the short penetration depth of soft X-rays means that the surface of the sample is receiving a higher radiation dose and heat load.

The results of this curve fitting are shown in Fig. 3. The points shown as solid diamonds represent the data points taken by spectral comparison, the open circles represent points taken using the single energy counting method. A non-linear least-squares fit to Eq. (1) yields a temperature of 0.55 ± 0.05 K. By using the following equation for thermal conductivity:

$$k(\Delta T) = \left(\frac{\dot{Q}}{\Delta T}\right)\cdot\left(\frac{l}{a}\right) \quad (2)$$

where a is the area and l is the length of the flow of heat, ΔT is the difference in temperature between the two sides of the sample and dQ/dt represents the heat flow with respect to time, a rough calculation can be performed for the thermal conductivity of the protein sample. Assuming that the total heat load impinging on the surface of the sample is on the order of ~10^2 μW and beam dimensions of ~5 mm^2 with an approximate sample thickness of

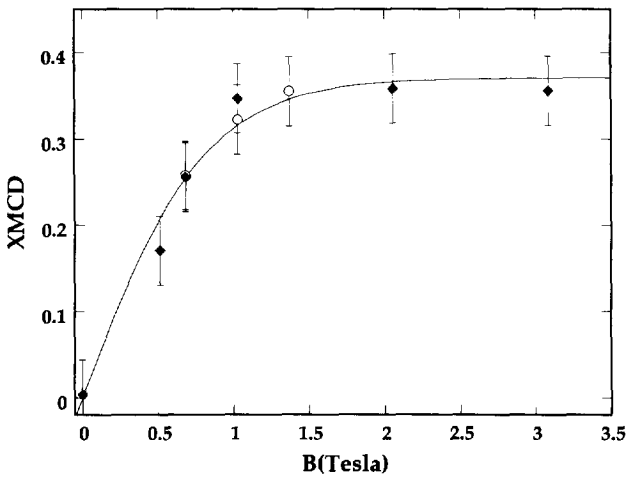

Fig. 3. The magnetization curve for Cu plastocyanin at a monitored temperature of ~300 mK. The solid black diamonds indicate data points derived directly from the individual data sets while the open circles are from data collected by the single energy counting method.

~50 μm, a thermal conductivity can be derived that is on the order of 10^{-2} mW (cm K)$^{-1}$. This value can be compared to the thermal conductivities at ~1 K for high purity copper metal, ~7 × 10^3 mW (cm K)$^{-1}$ and stainless steel, ~10^{-1} mW (cm K)$^{-1}$ [22]. For the energies used in these experiments, the photon flux of ~10^{11} photons s^{-1} only introduces ~15 μW to the overall sample heat load. As new insertion devices are commissioned which promise substantial increases in photon flux, this contribution will rapidly become very important in calculations of this type.

4. Summary

These results have established that XMCD can be recorded in modest magnetic fields at temperatures <1 K. This sets the foundation for further experiments on more complex systems. Magnetization curves of $S = 1/2$ systems establish a precise temperature at the surface of the sample and can be used as a calibration for future experiments. By using lower magnetic fields, there is less interference with fluorescence detection equipment and maximum signal throughput. These are critical factors in experiments on dilute metalloprotein systems. Ultra-low temperature XMCD should allow characterization of very weakly coupled magnetic systems.

Acknowledgements

We would like to thank Dr. Roger Carr for his help with the set-up and operation of the EPU. Experimental assistance from Fred Coffman, Dr. Jie Chen, Xin Wang, and Craig Bryant is gratefully acknowledged. This research was supported by the National Science Foundation grants DMB-9107312, DIR-9105323, DIR-9317942 (to S.P.C.) and CHE-9217628 (to E.I.S.), NIH grant GM-44380 (to S.P.C.) and support from the Department of Energy, Office of Health and Environmental Research. The Stanford Synchrotron Radiation Laboratory is supported by the Department of Energy, Office of Basic Energy Sciences.

References

[1] B.T. Thole, G. Van der Laan and G.A. Sawatzky, *Phys. Rev. Lett., 55* (1985) 2086.
[2] G. van der Laan, B.T. Thole, G.A. Sawatzky, J.B. Goedkoop, J.C. Fuggle, J.-M. Esteva, R. Karnatak, J.P. Remeike and H.A. Dabkowska, *Phys. Rev. B, 34* (1986) 6529.
[3] G. Van der Laan and B.T. Thole, *Phys. Rev. B, 43* (1991) 13401.
[4] (a) F. Sette, C.T. Chen, Y. Ma, S. Modesti and N.V. Smith, *AIP Conf. Proc., 215* (1990) 787. (b) P. Rudolf, F. Sette, L.H. Tjeng, G. Meigs and C.T. Chen, *J. Magn. Magn. Mater. 109* (1992) 109.
[5] J. VanElp, S.J. George, J. Chen, G. Peng, C.T. Chen, L.H. Tjeng, G. Meigs, H.-J. Lin, Z.H. Zhou, M.W.W. Adams, B.G. Searle and S.P. Cramer, *Proc. Natl. Acad. Sci. USA, 90* (1993) 9664.
[6] (a) E.I. Solomon, M.J. Baldwin and M.D. Lowery, *Chem. Rev., 92* (1992) 521. (b) S.K. Chapman in R.W. Hay, J.R. Dilworth and K.B. Nolan (eds.), *Perspectives in Bioinorganic Chemistry.* JAI Press, London, 1991, p. 95ff. (c) H.B. Gray and E.I. Solomon, in T.G. Spiro (ed.), *Copper Proteins.* Wiley, New York, 1981, p. 3ff.
[7] K.W. Penfield, R.R. Gay, R.S. Himmelwright, N.C. Eickman, V.A. Norris, H.C. Freeman and E.I. Solomon, *J. Am. Chem. Soc., 103* (1981) 4382.
[8] J.M. Guss, H.D. Bartunk and H.C. Freeman, *Acta Crystallogr., B48* (1992) 790.
[9] (a) D.R. McMillin, R.C. Rosenberg and H.B. Gray, *Proc. Natl. Acad. Sci. USA, 71* (1974) 4762. (b) D.R. McMillin, R.A. Holwerda and H.B. Gray, *Proc. Natl. Acad. Sci. USA, 71* (1974) 1339. (c) E.I. Solomon, J. Rawlings, D.R. McMillin, P.J. Stephens and H.B. Gray, *J. Am. Chem. Soc., 98* (1976) 8046.
[10] K.W. Penfield, A.A. Gewirth and E.I. Solomon, *J. Am. Chem. Soc., 107* (1985) 4519.
[11] S.J. George, M.D. Lowery, E.I. Solomon and S.P. Cramer, *J. Am. Chem. Soc., 115* (1993) 2968.
[12] P. Carra, *Jpn. J. Appl. Phys., S32* (1993) 279.
[13] B.T. Thole, P. Carra, F. Sette and G. Van der Laan, *Phys. Rev. Lett., 68* (1992) 1943.
[14] M. Altarelli, *Phys. Rev. B, 47* (1993) 597.
[15] M.-A. Arrio, Ph. Sainctavit, C. Brouder and C. Deudon, *Physica B, 208&209* (1995) 27.
[16] S.J. George, J. VanElp, J. Chen, G. Peng, S. Mitra-Kirtley, O.C. Mullins and S.P. Cramer, in B. Chance, J. Deisenhofer, S. Ebashi, D.T. Goodhead, J.R. Helliwell, H.E. Huxley, T. Iizuka, J. Kirz, T. Mitsui, E. Rubenstein, N. Sakabe, T. Sasaki, G. Schmahl, H.B. Stuhrmann, K. Wüthrich and G. Zaccai (eds.), *Synchrotron Radiation in the Biosciences.* Oxford University Press, New York, 1994, p. 313.
[17] W.L. Ellefson, E.A. Ulrich and D.W. Krogmann, *Methods Enzymol., 69* (1980) 223.
[18] R.Z. Bachrach, R.D. Bringans, B.B. Pate and R.G. Carr, *SPIE Proc., 582* (1985) 251.
[19] S. Lidia, R. Carr, *Nucl. Instrum. Methods, A347* (1994) 77.
[20] (a) C.T. Chen, F. Sette and N.V. Smith, *Appl. Opt., 29* (1990) 4535. (b) C.T. Chen, *Rev. Sci. Instrum., 63* (1992) 1229.
[21] S.P. Cramer, J. Chen, S.J. George, J. VanElp, J. Moore, O. Tensch, J. Colaresi, M. Yocum, O.C. Mullins and C.T. Chen, *Nucl. Instrum. Methods, A319* (1992) 285.
[22] For general discussion see: A. Kent, *Experimental Low Temperature Physics*, Macmillan Press, London, 1993.
[23] C. Kittel, *Introduction to Solid State Physics*, Wiley, New York, 1986, p. 401.